A reconnaissance study of ^{13}C-^{13}C clumping in ethane from natural gas

Matthieu Clog[a,*], Michael Lawson[b], Brian Peterson[c], Alexandre A. Ferreira[d], Eugenio V. Santos Neto[d], John M. Eiler[a]

[a] *California Institute of Technology, 1200 E California Boulevard CA91125 Pasadena, USA*
[b] *ExxonMobil Research, Houston, Texas, USA*
[c] *ExxonMobil Corporate Strategic Research, Annandale, New Jersey, USA*
[d] *Division of Geochemistry, PETROBRAS Research and Development Center (CENPES) PETROBRAS, Rua Horácio Macedo, 950, Ilha do Fundão Rio de Janeiro RJ 21941-915, Brazil*

Abstract

Ethane is the second most abundant alkane in most natural gas reservoirs. Its bulk isotopic compositions ($\delta^{13}C$ and δD) are used to understand conditions and progress of cracking reactions that lead to the accumulation of hydrocarbons. Bulk isotopic compositions are dominated by the concentrations of singly-substituted isotopologues ($^{13}CH_3$-$^{12}CH_3$ for $\delta^{13}C$ and $^{12}CDH_2$-$^{12}CH_3$ for δD). However, multiply-substituted isotopologues can bring additional independent constraints on the origins of natural ethane. The $^{13}C_2H_6$ isotopologue is particularly interesting as it can potentially inform the distribution of ^{13}C atoms in the parent biomolecules whose thermal cracking lead to the production of natural gas. This work presents methods to purify ethane from natural gas samples and quantify the abundance of the rare isotopologue $^{13}C_2H_6$ in ethane at natural abundances to a precision of $\pm 0.12‰$ using a high-resolution gas source mass spectrometer. To investigate the natural variability in carbon-carbon clumping, we measured twenty-five samples of

*Corresponding author, current address: SUERC, East Kilbride, United Kingdom
Email address: clog@caltech.edu (Matthieu Clog)

thermogenic ethane from a range of geological settings, supported by two hydrous pyrolysis of shales experiments and a dry pyrolysis of ethane experiment. The natural gas samples exhibit a range of 'clumped isotope' signatures ($\Delta^{13}C_2H_6$) at least 30 times larger than our analytical precision, and significantly larger than expected for thermodynamic equilibration of the carbon-carbon bonds during or after formation of ethane, inheritance from the distribution of isotopes in organic molecules or different extents of cracking of the source. However we show a relationship between the $\Delta^{13}C_2H_6$ and the proportion of alkanes in natural gas samples, which we believe can be associated to the extent of secondary ethane cracking. This scenario is consistent with the results of laboratory experiments, where breaking down ethane leaves the residue with a low $\Delta^{13}C_2H_6$ compared to the initial gas. Carbon-carbon clumping is therefore a new potential tracer suitable for the study of kinetic processes associated with natural gas.

Keywords: Clumped isotopes, Ethane, High-resolution mass spectrometry, Natural gas

1. Introduction

Ethane is the second most abundant component of natural gas after methane, generally accounting for a few percent by volume (Schoell, 1983). As a precursor for the generation of ethene, it is critically important for the petrochemical industry. Measurements of the ethane abundance in air also provide an important means of tracing emissions of thermogenic natural gases to the atmosphere, thus indirectly constraining contributions of such sources to the atmospheric methane (Rudolph, 1995).

The carbon and hydrogen isotopic compositions of low-molecular weight alkanes are key to our understanding of the generation and subsequent evolution of both oil and natural gas, as the mechanisms and conditions of production, transport and destruction of these molecules can cause distinctive isotopic fractionations. Previous interpretations of the bulk δ^{13}C and δD of ethane have focused on the tendency of both of these values to increase with increasing maturation of oil and gas reservoirs (i.e., evolution in chemistry due to sustained high temperatures). The most sophisticated of these interpretations examine the contrast in δ^{13}C between ethane and co-existing alkanes (particularly methane and propane), as diminishing differences between these species is a more reliable measure of thermal maturation than the δ^{13}C of any one taken alone (Chung et al., 1988; Whiticar, 1994; Prinzhofer and Huc, 1995). More recently, both carbon and hydrogen isotopic composition patterns of light alkanes are thought to be indicative of reaction with aqueous fluids and/or cracking (destruction by chemical reactions in response to heating) of longer alkanes — so called secondary cracking (Burruss and Laughrey, 2010; Zumberge et al., 2012). Despite their usefulness, stable isotopes do not necessarily provide unique interpretations. Competing models coexist due to the potential for various sources and the range of different physical processes that can affect natural gases. For example, cracking of kerogen is often understood as a kinetically-driven, irreversible process (Chung et al., 1988; Tang et al., 2000), while Mango (1996) advocated that trace-element catalysts might permit inter-molecular isotopic exchange among light alkanes, during or after formation.

In order to bring new constraints on the geochemistry of natural gas, we

turn to molecules containing two or more rare isotopes (called 'clumped isotopologues' or 'multiply-substituted isotopologues', Eiler, 2007). They have different chemical and physical properties from the unsubstituted or singly-substituted isotopologues. For many molecules, when the population of all co-existing isotopologues reaches thermodynamic equilibrium, the clumped isotopologues are more abundant than one would expect for a random distribution of isotopes, and this excess is generally controlled by temperature. It is therefore possible to use clumped isotopes as geothermometers (Wang et al., 2004). Moreover, physical- and chemical-kinetic processes can also fractionate clumped isotopologues to produce distinctive signatures (Eiler, 2013). Clumped isotopes have been studied previously in CO_2 both from the atmosphere (Eiler and Schauble, 2004; Affek and Eiler, 2006; Affek et al., 2007) and extracted from carbonate minerals (Ghosh et al., 2007; Eiler, 2011), in atmospheric O_2 (Yeung et al., 2012) and in methane from thermogenic and biogenic origins (Stolper et al., 2014a,b).

In particular, the study of ^{13}C-^{13}C clumping in ethane (i.e. the abundance of $^{13}C_2H_6$) could add to our understanding of the processes affecting natural gas formation, migration and chemical transformations occurring after formation. In the previous example of irreversible cracking versus inter-molecular isotopic exchange, differences in carbon-carbon clumping of ethane would be expected. If the second scenario is correct and catalytic exchange is sufficient to reach equilibrium, the clumped isotopes of ethane would reflect the temperature of formation of ethane. However, if the first scenario is correct, the clumped isotopes of ethane would reflect the isotope effects of the cracking reaction and the distribution of isotopes in the kerogen.

Moreover, the isotopes in biosynthetic organic molecules, and presumably in kerogen formed from biomolecules, are not randomly distributed (Abelson and Hoering, 1961; DeNiro and Epstein, 1977; Monson and Hayes, 1982), raising the possibility that cracking of kerogen will sample non-statistical populations of adjacent carbon atoms in source compounds, impacting the proportions of clumped isotope species. As different kerogen types have different proportions of organic molecule types (Vandenbroucke and Largeau, 2007), it is imaginable that the clumped isotope composition of ethane could serve as a fingerprint for the chemistry of source kerogens.

Natural gas geochemistry does not stop after the production of the alkanes: Diffusion (Prinzhofer and Pernaton, 1997), mixing between gases with different sources and isotopic compositions (Prinzhofer and Pernaton, 1997; Martini et al., 1998), biological oxidation (Martini et al., 1998), and thermal cracking of ethane itself (Burruss and Laughrey, 2010) are all significant factors influencing the abundance of ethane in natural gas and fractionating the different isotopologues of ethane in different ways. Specific processes can lead to coupled variations in bulk and clumped isotopes compositions, as previously shown for CO_2 (Eiler and Schauble, 2004) and CH_4 (Stolper et al., 2015).

The common techniques used to measure the bulk isotopic compositing of ethane (combustion to CO_2 to measure the $\delta^{13}C$ or pyrolysis to H_2 to measure the δD) are inadequate to measure carbon-carbon clumping. During the chemical reactions the distribution of isotopes among the different isotopologues (Table 1) is lost. Instead, in this study, we present a technique for the measurement of the abundances of four isotopologues of ethane

($^{12}C_2H_6$, $^{13}CH_3$-$^{12}CH_3$, $^{12}CDH_2$-$^{12}CH_3$ and $^{13}C_2H_6$) by mass spectrometry, using intact ethane as an analyte, without prior chemical transformation. This is enabled by a high resolution isotope ratio mass spectrometer, the MAT 253 Ultra (Eiler et al., 2013). This paper present the results of the application of this new mass spectrometric method to a suite of ethane samples (n=25) from natural gases of different geological origins, and the implications for our understanding of natural gas processes.

2. Clumped isotope notations for ethane

The theory, definitions of common reference frames, and earlier work on clumped isotope geochemistry have been reviewed previously (Wang et al., 2004; Eiler, 2007, 2011, 2013). Standard practice in this field is to report abundances of clumped isotopic species as enrichments or depletions with respect to the abundance that would be expected for a random, or 'stochastic', distribution of isotopes among all possible isotopologues (reported in units of‰, using the Δ symbol). The predicted stochastic abundance of $^{13}C_2H_6$ is equal to $[^{13}C]^2[H]^6$, where $[^{13}C]$ and [H] refer to the concentration of these isotopes as a fraction of all carbon atoms or hydrogen atoms, respectively. For the $^{13}C_2H_6$ isotopologue, we define $\Delta^{13}C_2H_6$ as follows :

$$\Delta^{13}C_2H_6 = 1000 \text{ x } ({}^{13C_2H_6}R_{measured} / {}^{13C_2H_6}R^* - 1)$$

where $^{13C_2H_6}R$ refers to the ratio of $^{13}C_2H_6$ to the unsubstituted isotopologue $^{12}C_2H_6$, and R* refers to the abundance ratio expected for a stochastic distribution of all isotopes among all possible isotopologues, based on the known bulk isotopic composition ($\delta^{13}C$ and δD values) of the sample. Most measurements of bulk isotopic content assume that unsubstituted and

singly-substituted isotopologues are present in their stochastic proportions, and thus calculated Δ values are often, strictly speaking, based on an internal inconsistency. However, this assumption leads to no meaningful errors for most natural isotopic compositions except when multiply substituted species exhibit extraordinary enrichments (Wang et al., 2004).

3. Methods and samples

3.1. Rationale

Our aim is to measure the proportion of molecules in a sample of ethane that contain two ^{13}C atoms, and if we are to interpret this measurement as a clumped isotope anomaly we must also know the full inventory of ^{13}C atoms in the sample (i.e., the δ^{13}C value). We do so using a high-resolution mass spectrometer, the Thermo Scientific IRMS-253 Ultra, or 'Ultra', located in the GPS Division of the California Institute of Technology and described in detail in Eiler et al. (2013). For this study, the critical properties of this instrument are that it is a dual inlet, gas source multi-collector, meaning it can achieve high levels of precision and accuracy relative to a chosen standard, and that it achieves a high mass resolving power, routinely ≈23,000 (compared to ≈200 for a classical IRMS instrument). This is sufficient to separate $^{13}C^{12}CH_6^+$ from $^{12}C_2DH_5^+$, and $^{13}C_2H_6^+$ from $^{13}C^{12}CDH_5^+$.

3.2. Description of the analytical procedures

We describe here succinctly how the measurements are performed during a typical day. Due to the presence of molecular fragments ($C_2H_5^+$ ions that can be substituted with heavy isotopes) and methanol ions on mass 32, a

complex ion and background correction scheme is necessary and it is fully detailed in the supplementary material (SI). The reference gas (CIT-Ethane-1) was sampled from a high purity gas cylinder purchased from Air Liquide. Its carbon isotopic composition was calibrated at PEERI ($\delta^{13}C$ = -24.50 ‰ vs PDB), and its hydrogen isotopic composition was calibrated at the California Institute of Technology ((δD = -109.0 ‰ vs SMOW), using conventional methods described in a later part of this article. The typical sample size is 50 micro-moles of ethane, and one full measurement takes about 7 hours.

3.2.1. Measurement 1 : sum of singly-substituted isotopologues and $^{13}C_2H_6$

We first configure the detector array of the Ultra to measure simultaneously the ratios of

$(^{13}C_2H_6^+ + {}^{12}CH_3OH^+)$ to $(^{12}C_2H_6^+ + {}^{13}C^{12}CH_5^+ + {}^{12}C_2DH_4^+)$

and

$(^{13}C^{12}CH_6^+ + {}^{12}C_2DH_5^+ + {}^{13}C_2H_5^+ + {}^{13}C^{12}CDH_4^+)$ to $(^{12}C_2H_6^+ + {}^{13}C^{12}CH_5^+ + {}^{12}C_2DH_4^+)$.

The methanol ion contributions are removed by background correction, and the contributions from fragments are corrected during the data processing using the fragmentation rate F (described in the SI). The contributions from $^{12}C_2D_2H_3^+$ are neglected due to its very low abundance. The differences between the sample and the reference are described using δ notation, with

$$\delta^{13}C_2H_6 = 1000 \; . \; ({}^{^{13}C_2H_6}R_{sample}/{}^{^{13}C_2H_6}R_{reference} \text{ -1})$$

and

$$\delta 31_1 = 1000 \; . \; ({}^{^{13}C^{12}CH_6 \, + \, {}^{12}C_2DH_5 \, + \, {}^{13}C_2H_5 \, + \, {}^{13}C^{12}CDH_4}R_{sample}/ \; {}^{^{13}C^{12}CH_6 \, + \, {}^{12}C_2DH_5 \, + \, {}^{13}C_2H_5 \, + \, {}^{13}C^{12}CDH_4}R_{reference} \text{ -1})$$

where ${}^{i}R$ is equal to

$i^+/({}^{12}C_2H_6^+ + {}^{13}C^{12}CH_5^+ + {}^{12}C_2DH_4^+)$

In order to get the desired precision for $\Delta^{13}C_2H_6$ (≈0.12‰), we run 10 acquisition blocks. Each of these is composed of 8 cycles with 33 seconds of integration time and 30 seconds of idle time. The precision is limited by counting statistics (Figure S5a in the SI).

3.2.2. Measurement 2: ^{13}C-substituted isotopologue

For the second measurement, the detector array is configured to measure the ratio of $({}^{13}C^{12}CH_6^+ + {}^{13}C_2H_5^+ + {}^{13}C^{12}CDH_4^+)$ to $({}^{12}C_2H_6^+ + {}^{13}C^{12}CH_5^+ + {}^{12}C_2DH_4^+)$, which involves moving one Faraday cup from its position in the configuration used for Measurement 1. The presence of fragments on both masses is corrected for during the data processing. The differences between the sample and the reference are noted, using the same δ and R notation as before, as:

$$\delta 31_2 = 1000 \cdot \left(\frac{{}^{13}C^{12}CH_6 + {}^{13}C_2H_5 + {}^{13}C^{12}CDH_4 R_{\text{sample}}}{{}^{13}C^{12}CH_6 + {}^{13}C_2H_5 + {}^{13}C^{12}CDH_4 R_{\text{reference}}} - 1 \right)$$

The measurements are organised in acquisitions blocks of 8 cycles, with 16 seconds of integration and 15 seconds of idle time. We usually perform 4 acquisitions, bringing the external error of the mean to ≈0.018‰.

By combining the two measurements, we are able to calculate the values and precisions of δD, δ^{13}C and $\Delta^{13}C_2H_6$ for a sample. The details of the calculation are provided in the SI. The precision reached is typically 0.02‰ for δ^{13}C, 0.5‰ for δD and 0.12‰ for $\Delta^{13}C_2H_6$. Our external errors in δ^{13}C and δD for a single sample analysis compare with state-of-the-art precision for conventional measurements of 0.1‰ and 2‰, respectively (Dai et al., 2012). The reduction in error associated with direct mass spectrometric analysis

of ethane means it will be difficult to prove whether or not the accuracy of our measurements (i.e., placement on some recognised interlaboratory scale, such as V-SMOW or V-PDB) is also better than the precision of conventional methods.

3.3. Sample handling and purification

Samples with high purity (typically >99% ethane) are required for the method we describe. Therefore we developed techniques to purify ethane from other gases, especially from other components from natural gases (other alkanes, N_2, CO_2, etc) by vacuum cryogenic separation. Although ethane has a low partial pressure (< 0.1 Pa) at the temperature of liquid nitrogen (77K), liquid nitrogen is not cold enough to separate methane from ethane without losing a significant portion of ethane (Slobod, 1951). Therefore, a helium-cooled cryostat (CTI-Cryogenics and Janis Research Co.) set at 20K is used to freeze all gases (except H_2 and He).

If the methane present in the sample is to be recovered for analysis, we follow the procedure described by Stolper et al. (2014a) before proceeding. Otherwise, the trap is set to 70K, allowed to equilibrate for a few minutes and then pumped for 2 to 5 minutes. To ensure that no methane is left frozen in the trap, the cold trap is heated to 95K, left to equilibrate for 2 minutes, then set to 70K, left to equilibrate for 2 minutes, and pumped again for 2 minutes. This step also removes N_2 and O_2 from the cold trap.

The next step is the separation of ethane from propane and carbon dioxide, which have similar vapour pressures at low temperature. The trap is set to 115K and left to equilibrate for 2 minutes. At this temperature, the saturation vapour pressure of ethane is equal to 167 Pa, while the vapour pressure

of propane and carbon dioxide are both ≈1 Pa. Gases evolved from the trap are condensed onto a trap cooled with liquid nitrogen (77K). Due to the differences in partial pressures, this concentrates ethane relative to propane and CO_2 into the 77K trap. After 1 to 5 minutes (depending on the amount of gas in the cryostat), the pressure falls sharply as the ethane is transferred to the $N_{2,l}$ trap. At this stage, the $N_{2,l}$ trap is closed. The cryostat is set to 150K, left to equilibrate for 2 minutes, and pumped for 5 minutes to remove all the propane and CO_2 than has not been transferred along with ethane to the $N_{2,l}$ trap. The cryostat is then set to 70K and the gases condensed in the $N_{2,l}$ trap are thawed and transferred back into the cryostat. This distillation procedure is repeated three more times. The resulting ethane aliquots are then condensed with liquid nitrogen into Pyrex break-seals. Those break-seals are later connected to the sample introduction inlet of the Ultra and cracked to expand the gas into the bellows. The procedure takes about 3.5 hours per sample (starting from natural gas mixtures).

We verified that our sample handling procedures were not modifying the isotopic composition of ethane (detailed in the SI).

3.4. Natural gas samples

3.4.1. Natural gas associated with oil

There are two sample suites coming from Brazilian basins, where natural gas is associated with oil in the reservoir rocks. Those are conventional hydrocarbon fields, where the products from kerogen cracking migrated from the source rock towards a reservoir rock. The first one is the Potiguar basin (7 samples), which formed during the early Cretaceous (de Matos, 1992). The source rocks have a mixture of lacustrine and deltaic origins (dos San-

tos Neto and Hayes, 1999; Prinzhofer et al., 2010). The second sample suite (5 samples) comes from the Sergipe-Alagoas basin, which also formed during the early Cretaceous and where source rocks have diverse origins, from lacustrine to deltaic to marine (Mello et al., 1988). Both sample suites were chosen to represent a range of natural gas compositions, thought a priori to correspond to differing degrees of progress of the cracking reactions in the kerogen (i.e., different degrees of maturity).

3.4.2. Shale gases suites

There are three sample suites coming from shales, all from the continental United States. For those three locations, the products of kerogen cracking were retained in the source rock.

The first suite (2 samples) comes from the Haynesville Shale, a Jurassic formation found in eastern Texas and western Louisiana (Hammes et al., 2011), which is thought to have experienced minimal uplift since the shale reached its maximum burial depth (Stolper et al., 2014b).

The second suite (3 samples) comes from the Pennsylvanian section of the Marcellus shale, which, in contrast, has been uplifted by more than 3km since its maximum burial. The Marcellus shale is Devonian in age (Lash and Engelder, 2011). For both of those locations, the wells sampled yielded gas, but no oil.

The third suite (8 samples) comes from the Eagle Ford shale in Texas, which is of Upper Cretaceous age (Robison, 1997), and exhibits a range in thermal maturity from the oil window through the gas window.

3.5. Laboratory experiments

3.5.1. Kerogen cracking

Two hydropyrolysis experiments were conducted with two different kerogen-rich rocks (a sample of Woodford Shale and a sample of an Albian/Aptian lacustrine shale from the Araripe basin in Brazil), following methods described in Lewan and Ruble (2002). The experiments in both cases were sequential: the samples were heated to a given temperature for 72 hours, the gases evacuated with aliquots collected for analysis, and then the samples were heated again at a greater temperature. For the Woodford Shale, the temperatures were 330, 360 and 390C, and for the Araripe shale 320, 340 and 360C. From the aliquots of gas collected from analysis, ethane samples were separated in a vacuum line and then measured as described previously in this paper.

3.5.2. Ethane pyrolysis

In this experiment, aliquots ($\approx$ 100 micromol) of ethane were introduced in empty silica tubes that were then sealed. The tubes were then put in a furnace held at 600C for either 4 or 8 hours. The tubes were then recovered and connected to a vacuum line. The ethane left in the tubes was isolated from the other reaction products using the methods presented above, measured by manometry to estimate the percentage of gas lost and then measured for its isotopic composition in δ^{13}C, δD and $\Delta^{13}C_2H_6$ as presented above.

4. Results

4.1. Experimental Reproducibility

We described earlier the internal precision from the measurements performed on the mass spectrometer, summarised as the standard error of a single sequence of acquisitions, including propagated errors in calculated $\Delta^{13}C_2H_6$ values. There are other potential sources of additional errors, for example variations of the instrument conditions, which are tested against here.

4.1.1. Within a session

Analytical sessions (i.e., periods of continuous measurements of ethane standards and samples) are typically 1 to 2 weeks long. We prepared an internal standard whose isotopic composition is distinct from our reference gas by mixing aliquots of pure ethane. This internal standard was measured 3 times in a single analytical session to check if there was some variability in the measured isotopic compositions (first rows of Table 2). We observe that the measured isotopic compositions are indistinguishable within 2σ of the nominal standard errors of each measurement, suggesting no additional sources of experimental error, at least over these short time periods.

4.1.2. Inter-session

We compare in Table 2 and Figure 1 measurements of our internal standard against the CIT-Ethane-1 reference gas over the course of 12 months. During these months, there were several operations that could potentially change the instrumental conditions including filament changes, venting of the ion source, and replacement of the high-resolution slit. In other clumped

isotopic systems, it is often critical to establish a reference frame to correct for changes in isotopic ratios (e.g., Dennis et al., 2011, for clumping in CO_2) between different analytical sessions (and between different laboratories — an issue we cannot yet evaluate for ethane). The measured values of $\Delta^{13}C_2H_6$ show remarkable constancy over time, with a standard deviation for the population of separate analyses equal to 0.08‰ (9 measurements). This is comparable to our estimated average standard error for one measurement (0.12‰). The long-term experimental reproducibility for $\delta^{13}C$ and δD are slightly worse than the standard error of a single measurement (respectively, 0.03 versus 0.02 and 0.66 versus 0.5). This suggests that there might be subtle fractionations, variations in reference gas composition or other long-term artefacts. However, these effects are a small multiple of analytical precision, substantially less than long-term precision of conventional measurements, and, if present, fractionate the isotopologues in a way that introduces no observable errors in $\Delta^{13}C_2H_6$.

4.2. Comparison with classical techniques

In order to test the accuracy of the bulk isotopic composition measured on ethane using our technique, we compared the values we measured on the Ultra to these obtained using well-established methods. For carbon isotopes, samples were measured at the Power Environmental Energy Research Institute (PEERI) or by Isotech. For hydrogen isotopes, samples were measured at the California Institute of Technology or by Isotech. We found that the bulk isotopic ratios measured using the Ultra exhibit no systematic errors with respect to those measured using conventional techniques (detailed in the SI).

4.3. Measurements of natural samples

4.3.1. Bulk isotope measurements

The δ^{13}C values range from -18.71 to -42.3‰ (vs PDB), while the δD range from -97.5 to -209.1‰ (vs SMOW), as reported in Table 3. The extreme values for δ^{13}C are found in shale gases, and the range in the Brazilian suites being restricted to -27.49 to -41.86‰. Those values are typical for ethane in natural gas (e.g., Prinzhofer and Huc, 1995), and the range was expected as the samples were selected to span various extent of gas maturity. This is also reflected in the variation in gas wetness (the molar ratio of sum of alkanes with 2 or more carbon atoms divided by the sum of all alkanes), ranging from 0.04 to 0.41. The samples from the Sergipe-Alagoas contain on average more methane than the samples from the Potiguar basin, and their bulk isotopic composition cover a smaller range clustered at the more isotopically enriched in heavy isotope end of the ranges (from -27.48 to -32.20‰).

The samples from the Eagle Ford suite are on average more rich in heavy isotopes than the Brazilian suites (δ^{13}C from -18.71 to -32.75‰ and δD from -99.4 to -159.0‰), but the gas wetness is similar, ranging from 0.04 to 0.30. In contrast, the samples from the Marcellus and the Haynesville shales do not display a large range of isotopic signatures and contain only low amounts of alkanes other than methane (gas wetness between 0.02 and 0.06).

4.3.2. Clumped isotopes

The $\Delta^{13}C_2H_6$ measured range from -4.0 to 0.83‰ compared to our standard (Table 3 and Figure 2). The total range (4.83‰) is more than 30 times larger than our analytical precision. The fact that the values measured on natural samples are within a few‰ of 0 suggests that our reference gas is

not exceptionally enriched or depleted in $^{13}C_2H_6$ compared to the stochastic distribution (or that all natural gases share a common enrichment or depletion). This is not a perfectly satisfying solution, but as explained in Appendix A calculation of the absolute clumping signature is not straightforward. It should also be noted that we observe a large range of clumping signatures compared to other clumped isotope systems: the whole observable range for clumped isotopes in carbonates is about 1‰ (Eiler, 2007), and although for methane the total range between stochastic distribution and samples equilibrated at ambient temperatures is about 7‰ (Stolper et al., 2014a), the range of clumping signatures observed in most thermogenic gases is less than 1‰ (Stolper et al., 2014b).

Individual suites, except the two samples from the Haynesville shale, also display ranges in $\Delta^{13}C_2H_6$ that are several times greater than our analytical precision. We observe more variability within the Potiguar samples (from -2.72 to +0.77‰) than within the Sergipe-Alagoas ones (from -0.51 to +0.25‰), the Eagle Ford suite (from -0.35 to + 0.83‰) or the Marcellus samples (from -4.0 to -0.7‰).

4.4. Laboratory experiments

The results from the laboratory experiments are summarised in Table 4.

4.4.1. Hydrous pyrolysis

For both source rocks, the $\delta^{13}C$ and δD of the evolved gas increases with temperature. This is consistent with the results of kinetic cracking models (e.g. Chung et al., 1988; Tang et al., 2005), where the earliest products are the most depleted in heavy isotopes compared to the kerogen. For the Woodford

Shale, the $\Delta^{13}C_2H_6$ increases by ≈0.4‰ as temperature increases from 330 to 390C, while in the gas evolved from the Araripe shale the reverse is observed, with a drop in $\Delta^{13}C_2H_6$ of ≈1‰ between 320 and 360C (Figure 3).

4.4.2. Ethane pyrolysis

The $\delta^{13}C$ of the residual ethane increase with the reaction time, which is expected for kinetically controlled breakdown of the ethane molecule. However, the $\Delta^{13}C_2H_6$ of the residual ethane is decreasing by close to 1.7‰ when there is 35% of the initial ethane left (Figure 4). Although unintuitive, this is not necessarily a surprising result, a similar behaviour can be observed in CO2 with diffusion (Eiler, 2007) where the $\delta^{13}C$ and $\delta^{18}O$ increase in the residue but the Δ_{47} decreases.

The δD also increases with reaction time (from -110.1 to +4.6‰). Part of this variation may be due to diffusion of H_2 through the silica tube. A potential pitfall of that experiment was creation of ethene, which is difficult to separate from ethane by cryogenic methods. We verified that the amount of ethene was null or negligible by comparing the ionisation spectra of our residual gas to that of pure ethane aliquots.

5. Discussion

In this section, we will discuss various relevant processes that could lead to the observed variations in clumping signatures in natural gas .

5.1. Standardisation and frame of reference

All of the species other than ethane that have been subject to significant clumped isotope study (CO_2, O_2, CH_4 and N_2O) can be driven to internal

isotopic equilibrium by heating (or, in the case of O_2, exposure to a spark discharge), either alone or exposed to a catalyst. For CO_2, oxygen exchange among CO_2 molecules or between CO_2 and water occurs on laboratory time scales at temperatures between 0 and 1000°C (Eiler and Schauble, 2004; Dennis et al., 2011), allowing the following reaction to reach equilibrium:

$$^{13}C^{18}O^{16}O + {}^{12}C^{16}O_2 = {}^{13}C^{16}O_2 + {}^{12}C^{18}O^{16}O$$

Similarly, for methane, activation of the carbon-hydrogen bond on a high-surface-area nickel catalyst (Stolper et al., 2014a) allows for the following homogeneous equilibrium to be reached:

$$^{13}CH_3D + {}^{12}CH_4 = {}^{13}CH_4 + {}^{12}CH_3D$$

For methane, carbon dioxide and other readily equilibrated molecules, it is therefore possible to experimentally create equilibrated distributions of isotopologues for a range of temperatures, and therefore to compare measured sample compositions to a reference frame tied to some known (or knowable) thermodynamic equilibrium condition. The measured values can then be compared to model predictions, e.g., following the work of Bigeleisen and Mayer (1947) and Urey (1947), which allow relatively confident calculation of the clumped isotope compositions of simple molecular gases relative to a stochastic reference frame (Wang et al., 2004).

We can write a similar reaction for ethane :

$$^{13}C_2H_6 + {}^{12}C_2H_6 = 2\times{}^{13}C^{12}CH_6$$

But for this reaction to reach equilibrium, the carbon-carbon bond of the ethane molecule needs to be repeatedly broken and reformed. At low pressures ($<$ 30 kbar), ethane is thermodynamically unstable relative to carbon plus methane or hydrogen (Kenney et al., 2002), meaning many reactions

that break the carbon-carbon bond in ethane are likely to be strongly irreversible at low pressures.

Ethane is thermodynamically unstable at the typical pressure and temperature conditions where it is generated in nature through hydrocarbon cracking or Fischer-Tropsch type reactions associated with serpentinization and, given enough time or access to catalysts, will convert to methane (Fu et al., 2007). The Fischer-Tropsch reactions (e.g. Berndt et al., 1996) that can generate ethane are irreversible, thus likely to express kinetic isotope effects, and so cannot be assumed to produce either an equilibrated or random distribution of isotopes. For these reasons, we have not been able to develop a reference frame for the study of ^{13}C-^{13}C clumping in ethane that involves comparison of measurements with an experimentally created random or equilibrated condition. Due to the low abundance of multiply-substituted isotopologues, calibrating a reference frame by analysing mixtures containing known amounts of labelled $^{13}C_2H_6$ (i.e., a 'standard additions' experiment) is not a viable solution due to technical constraints which are detailed in the appendix A.

The study of the clumped isotope compositions of metastable compounds such as ethane requires, at least provisionally, a relative reference frame involving standardisation to arbitrary reference standards, not unlike reference frames used in conventional isotope geochemistry. We report all of our clumped measurements relative to the reference gas mentioned above, 'CIT-Ethane-1'. Thus, the $\Delta^{13}C_2H_6$ values we report are not relative to a stochastic reference frame; rather, they are to a 'CIT-Ethane-1' reference frame. CIT-Ethane-1 itself, and any ethane sample that shares its state of isotopic

ordering, will exhibit $\Delta^{13}C_2H_6$ values of 0. We have no way to confidently estimate the $\Delta^{13}C_2H_6$ value of CIT-Ethane-1 in a stochastic reference frame, but we suspect it is within a few‰ of 0, as all natural samples are within a few permil of CIT-Ethane-1. Aliquots of this reference standard are available for use by other laboratories, on request to the authors. Repeated measurements of the internal standard were used to check for potential variations in scale compression with time.

5.2. Isotope exchange at equilibrium

We cannot yet anchor our measurements of $\Delta^{13}C_2H_6$ to a stochastic or thermodynamic reference frame due to the chemical properties of ethane, but it is worth considering the variations in clumped isotope composition of ethane from petroleum deposits, and whether they might be consistent with equilibrium variations at a range of formation or storage temperatures. It is not clear what we should expect. On one hand, as discussed earlier in 5.1, ethane is thermodynamically unstable within the relevant ranges in pressure and temperature, and is mainly created through irreversible reactions, which argues against reaching internal isotopic equilibrium at a given temperature. The bulk stable isotope compositions of ethane are generally considered to reflect kinetic isotope effects associated with irreversible cracking reactions (as in, for example, the model of Tang et al., 2000). On the other hand, Mango (1996) suggested that the cracking of organic matter was mediated by transition metal catalysts, and such mediation could allow for exchange of carbon atoms in molecules bearing several carbon atoms, perhaps leading to equilibration of clumped isotope compositions.

However, the range of $\Delta^{13}C_2H_6$ displayed (4.8‰) is more than 15 times

greater than the maximum range that could result from internal isotopic equilibrium at different temperatures (0.25 between 0 and 1000°C, Piasecki, 2015). This consideration alone suggests the ^{13}C-^{13}C clumping in ethane is unlikely to be a good thermometer for the temperature of formation of natural gas, even if it formed at thermodynamic equilibrium (unless errors in this analysis reach the ≈0.01‰ level, as for the Δ47 value of CO_2; Eiler and Schauble, 2004; Dennis et al., 2011). ^{13}C-^{13}C clumping in ethane from natural gas does not reflect equilibrium temperatures, and we have to investigate kinetic processes during or after formation of the ethane molecules, and inheritance from the ordering of heavy isotopes in the kerogen before cracking, as potential explanations.

5.3. Diffusion and mixing

Diffusion and mixing can modify the clumped signatures of gases (Eiler, 2007). We can calculate the magnitude of the modifications and therefore compare to our observations to see if those processes are going to play an important role in the interpretation of C-C clumping signatures in ethane.

During diffusion, the ratio of molecules with different masses will be changed. For Knudsen diffusion, where collisions with other molecules can be ignored, the fractionation factor is equal to the square root of the ratio of the masses. For ethane, it means the $\delta^{13}C$ of the diffused gas is ≈16‰ lighter than the residue. There are also less isotopologues of mass 32 in the diffused gas, but the $\Delta^{13}C_2H_6$ is actually increased by 0.5‰. If the diffusion conditions are different, and the ethane has to diffuse through a gas mainly composed of methane, which seems more relevant for natural gas samples, the expected fractionation is smaller ($\delta^{13}C$ decreased by 5.6‰ and $\Delta^{13}C_2H_6$

increased by 0.3‰). The magnitude of the changes in $\Delta^{13}C_2H_6$ that diffusion could cause are too small to explain most of the variation we observe. We would also expect a correlation between $\delta^{13}C$ and $\Delta^{13}C_2H_6$ if that was the case (see Figure 2a), and the range of $\delta^{13}C$ we see is too small compared to the range in $\Delta^{13}C_2H_6$ for diffusion to be the controlling process.

Mixtures of gases with the same initial $\Delta^{13}C_2H_6$ but a different $\delta^{13}C$ will exhibit excesses in their $\Delta^{13}C_2H_6$. However those excesses are small compared to the range we see in our samples. For example, if we mix gases with a $\Delta^{13}C_2H_6$ of 0 and $\delta^{13}C$ of respectively -25 and -45‰ (just over the range of $\delta^{13}C$ observed in our samples), the greatest excess in $\Delta^{13}C_2H_6$ created is only 0.1‰, too small to explain the variations in our suites.

5.4. Extent of kerogen cracking

One possibility is that the range in $\Delta^{13}C_2H_6$ comes from kinetic isotope effects associated with the breaking of carbon-carbon bonds in the kerogen to ethane and other products. In this case, ethane evolved from a single source may vary in $\Delta^{13}C_2H_6$ as a function of thermal maturity. It is previously established that the $\delta^{13}C$ of ethane varies with thermal maturity (e.g., Chung et al., 1988), and so if this factor dominates we would expect to see a well-defined correlation between $\Delta^{13}C_2H_6$ and $\delta^{13}C$. No such correlation is observed (Figure 2a). Moreover, in this case we might expect to see a correlation between $\Delta^{13}C_2H_6$ and other independent measures of thermal maturity, such as methane formation temperature (Stolper et al., 2014b). As shown on Figure 2b, no such correlation is observed.

5.4.1. Maximum effect on clumping from kinetic fractionation

Although we see no empirical evidence for a relationship between $\Delta^{13}C_2H_6$ and source thermal maturity, it is also useful to predict what such a relationship might look like. We make a first estimate using the following simple model: ethane is created by cleaving at least one carbon-carbon bond in a molecule of the source kerogen. In the simplest case considered by previous models (Chung et al., 1988; Tang et al., 2000), this process can be approximated as cleavage of a C-C bond in an n-alkane, between the C2a and C2b positions (i.e., the second and third carbons from the end of that precursor). The primary kinetic isotope effect expected in such a reaction is a reduction in the rate of reaction when an atom of ^{13}C is present in either of these two positions. The C2a position will be transferred to the product ethane, and thus we expect that product to be lower in $\delta^{13}C$ than its source, by half the magnitude of the kinetic isotope effect (because the methyl position of the precursor is also transferred to the product ethane, but without a primary kinetic isotope effect).

There are three factors that can contribute to the $\Delta^{13}C_2H_6$ value of the ethane produced by this process: (1) non-statistical distribution of ^{13}C between the methyl and C2a sites of the precursor compound (i.e., the $\Delta^{13}C_2H_5$ value of the CH_3—CH_2—... group at the end of that n alkane); (2) the relative sizes of the kinetic isotope effects for the reactant species: $^{13}CH_3$—$^{12}CH_2$—..., $^{12}CH_3$—$^{13}CH_2$—... and $^{13}CH_3$—$^{13}CH_2$—...; and (3) the absolute value of the kinetic isotope effect for the species, $^{12}CH_3$—$^{13}CH_2$—... This third effect is somewhat counter-intuitive and bears further explanation. If we consider the simplified case that ^{13}C is randomly distributed across the

relevant sites of the reactant precursor, no secondary isotope effects associated with ^{13}C substitution in the terminal methyl site of that precursor, (KIE for $^{13}CH_3$—$^{12}CH_2$—... is 1), and a KIE for $^{13}CH_3$—$^{13}CH_2$—... that is the same as that for $^{12}CH_3$—$^{13}CH_2$—..., one might expect no clumped isotope effect associated with the cracking reaction. However, one will still occur because the product ethane will contain two carbon atoms that are symmetrically equivalent but come from different precursor sites that had different kinetic isotope effects during ethane formation. That is, the final ethane is chemically symmetrical, but composed of one pool of carbon atoms that is, on average, high in $\delta^{13}C$ (those inherited from the terminal methyl site in the precursor) and a second pool of carbon atoms that is, on average, lower in $\delta^{13}C$ (those inherited from the C2a site, but with a kinetic isotope effect). The molecular concentration of ^{13}C will be the average of these two pools, and the symmetric equivalence of the two C sites will lead one to predict a probability of forming $^{13}C_2H_6$ to be proportional to the square of that average concentration. But in fact, the probability of forming $^{13}C_2H_6$ will be proportional to the product of the ^{13}C concentration in the first pool times the ^{13}C concentration in the second. I.e., with A the concentration of ^{13}C in the initial molecule of kerogen and those assumptions,

$[^{13}C]$ of pool 1 = A

$[^{13}C]$ of pool 2 = B, with B<A due to the KIE of cracking

$[^{13}C]$ for full molecule = (A+B)/2

$[^{13}C_2H_6]$ for the stochastic distribution is proportional to $[(A+B)/2]^2$

$[^{13}C_2H_6]$ for the sample is proportional to (A)x(B)

For common values of A (near 0.01) and plausible values of the KIE

(≈0.98), it is easy to show that this circumstance results in $\Delta^{13}C_2H_6$ values of product ethane that are always lower than the equivalent $\Delta^{13}C_2$ value of the two relevant sites in the precursor. This effect can be thought of as analogous to the sampling-statistics effects on clumped isotope compositions that are well recognised to arise from mixing (Eiler and Schauble, 2004; Eiler, 2007, 2011, 2013) and are hypothesised to result from photosynthetic assembly of the O_2 molecule from two separate oxygen pools (Yeung, 2016).

The effects discussed above may be important for ethane in some contexts, and the principles involved may matter in other isotopic systems. However, for plausible values of the KIE associated with cracking a precursor to form ethane, the maximum range in $\Delta^{13}C_2H_6$ between the earliest formed ethane and the last is only ≈0.15‰. This is not enough to explain our findings for natural gases.

5.4.2. Hydrous pyrolysis data

The sequential hydrous pyrolysis experiments inform us on the variations in the composition of the cracking reaction products with greater extent of cracking. It is worth noting that in those experiments the gas was removed at each step, and each measurement corresponds to gas produced on a narrow temperature window, possibly through different reaction pathways or from different precursor molecules in the kerogen. Natural samples, on the other hand, are the result of the accumulation of all the gases produced from the onset of cracking, except if gas loss occurs during migration or storage, and their compositions will represent the weighted average of the various products of the cracking reactions.

In the Woodford shale experiment, the $\Delta^{13}C_2H_6$ decreases with increas-

ing temperature, which is consistent with the simple model described above, where the first products are the most depleted in heavy isotopologues. However the magnitude observed ($\approx$ 0.4‰) is greater than the one expected ($\approx$0.15‰ at most). For the Araripe shale however we see the reverse happening, with the later products having a lower $\Delta^{13}C_2H_6$. This may be the results of different ethane precursors in the two source rocks, or differences in the relative contribution of kerogen and oil cracking for the formation of ethane. A key insight however is that cracking reaction can produce a diversity of $\Delta^{13}C_2H_6$ depending on the source rock and on the degree of maturation of the kerogen. Additionally, the model of Mango (1996), with the potential for carbon exchange on catalysts in the source rocks, is shown to be inconsistent with the range of $\Delta^{13}C_2H_6$ produced by the hydrous pyrolysis experiments, at least over a laboratry timescale.

5.5. Inheritance from the source

The previous section highlighted that an unequal $\delta^{13}C$ between the two carbon atoms can create variations in the $\Delta^{13}C_2H_6$ values. We have considered above the consequences of the isotopic fractionation starting from an isotopically homogeneous source, but this is not necessarily the case. We know from previous studies that ^{13}C is not distributed randomly among non-equivalent carbon sites in many organic molecules, with $\delta^{13}C$ differences between neighbouring carbon atoms of up to 20‰ (Abelson and Hoering, 1961; DeNiro and Epstein, 1977; Monson and Hayes, 1982; Gilbert et al., 2012). Such differences are likely to be recorded in the kerogens during burial of the organic matter, as the chemistry of the kerogen partly reflect that of the buried organic matter (Vandenbroucke and Largeau, 2007). In the Potiguar

basin, moreover, there are source rocks of both lacustrine and marine types (Prinzhofer et al., 2010). As the organic matter buried in those environment is going to differ in chemical compositions (for example, the proportions of lipids, proteins and cellulose Vandenbroucke and Largeau, 2007), there are potentially differences in the distribution of heavy isotopes in the kerogens of the different source rocks. We can calculate the maximum effect created by those isotopic contrasts in the kerogen as we did before for the kinetic effect. The difference between the ethane from a source where the terminal carbon is enriched by 20‰ in $\delta^{13}C$ compared to the second carbon and one from a source with homogeneous $\delta^{13}C$ is ≈0.1‰, assuming identical amounts of maturation. With this simple model, the greatest $\Delta^{13}C_2H_6$ contrast that can be obtained from the combination of heterogeneous $\delta^{13}C$ in two distinct sources and extremely different extents of thermal maturation would be ≈0.5‰, only one eighth of the total range observed in our samples.

We observe a greater difference that this theoretical prediction in the Araripe shale for ethanes produced at different temperatures by hydrous pyrolysis. One possibility could be the existence of several types of precursors that can produce ethane and contribute at different temperatures, or possibly changes in the percentage of the ethane coming from secondary cracking of oil. In any case, the range of $\Delta^{13}C_2H_6$ in natural gas samples is greater than what can be explained by source inheritance and/or cracking processes. The variations in $\Delta^{13}C_2H_6$ indicates that the ethane in the gas is altered after cracking occurs, beyond what can be accounted for by diffusion or mixing processes.

5.6. Gas wetness: indicative of secondary cracking of ethane?

For both Brazilian basins and the Eagle Ford shale, samples with lower wetness, i.e., where the gas contains more methane relative to other alkanes, have lower clumping signatures (Figure 5). The shale gases from Haynesville and Marcellus, which also display low wetness, also display some of the lowest $\Delta^{13}C_2H_6$ of our sample suite. There are differences between the basins: the Potiguar basin samples are wetter and their $\Delta^{13}C_2H_6$ are lower at a given wetness than the samples from Sergipe-Alagoas. Moreover, in the Sergipe-Alagoas basin there is a strong correlation between the two parameters, while for the Potiguar suite the data points form a triangular wedge pointing towards low wetness and low $\Delta^{13}C_2H_6$ values. This could be related to the greater variability of the samples from the Potiguar suite.

For those three sample suites, this means that the process creating the range of $\Delta^{13}C_2H_6$ values is also related to the variations in the relative ratio of methane to ethane (and other light alkanes). The lowest values observed for the Marcellus and Haynesville samples could result from the same process driven to greater extents. One potential explanation is that ethane is destroyed by catagenetic reactions after its initial formation, driving changes in the clumping signature of the residual gas, similar to the ethane pyrolysis experiment that we performed. In those experiments, $\Delta^{13}C_2H_6$ decreased by -1.7‰ after 65% of the original ethane had been lost (Figure 4). There should be variations in $\delta^{13}C$ associated with the secondary destruction of ethane, but it is difficult at this stage to gauge their magnitude (relative to the magnitude of the $\Delta^{13}C_2H_6$ change) with our experimental data. Assuming 1) that our experiment is representative of the fractionations occurring

during ethane breakdown in natural reservoirs and 2) Rayleigh distillation, we illustrate the resulting trend in Figure 5 (dotted line). The exact shape of this trend may vary in natural reservoirs depending on the fate of the products of the reaction, e.g. if each molecule of ethane is turned into methane the slope would be steeper. Destruction of 80 to 90% of the initial ethane could explain well the variations we observe in the sample suites, although at this stage we cannot exclude more complex scenarios, for example multi-stage cracking.

In the three large sample suites, the gas is associated with oil. The temperatures measured using methane clumped isotopes (which are formation temperatures) range from 157 to 221°C in the Potiguar suite. This is thought to be compatible with oil cracking (Clayton, 1991). However a previous study (Prinzhofer et al., 2010) in the Potiguar basin concluded that the alkanes heavier than methane were formed through primary cracking. It is possible that there is decoupling between the methane and the other alkanes (e.g., through biodegradation or diffusion). The temperatures measured on methane for the Marcellus and Haynesville samples are in the range 179-207°C, and from our results at least 80% of the ethane has been destroyed, while studies like Burruss and Laughrey (2010) place the onset of gas cracking around 250°C.

In this discussion section, we have shown that the carbon-carbon clumping signature of natural samples was not recording equilibrium formation or storage temperatures, but kinetic processes with possibly a small contribution from inheritance of the distribution of isotopes in the molecules in the kerogen. Although we have so far only a few samples and lack the rich and

varied data available for the interpretation of bulk isotopic compositions of alkanes, we have shown that ethane, and presumably the other light alkanes too, is affected by processes other than just diffusion or mixing after cracking. We propose the following scenario: ethane destruction is taking place, at a lower temperature than predicted in previous studies and that this process is behind the observed ranges in $\Delta^{13}C_2H_6$ and gas wetness. Low $\Delta^{13}C_2H_6$ values measured for shale gases samples which are methane-rich are consistent with this scenario.

6. Conclusion

We developed a method to measure simultaneously the bulk isotopic composition (δ^{13}C and δD) and the relative amount of $^{13}C_2H_6$ with a high resolution mass spectrometer, with long-term reproducibility on the order of 0.1‰. The bulk isotopic compositions obtained by this technique exhibit no systematic differences from those obtained from conventional techniques. Although we cannot anchor our measurements of $\Delta^{13}C_2H_6$ to a reference frame based on thermodynamic equilibrium, we show that ethane from various hydrocarbon systems exhibits variations in $\Delta^{13}C_2H_6$ are approximately 30 times larger than our analytical precision and at least 15 times larger than the range plausibly associated with equilibrium over some range in geological temperatures.

This finding suggests that the ^{13}C-^{13}C clumped isotope compositions of natural ethanes are controlled by chemical-kinetic isotope effects or inheritance from the organic molecules of the kerogen. Physical processes like diffusion or mixing can only create small variations in $\Delta^{13}C_2H_6$. In the sam-

ple suites presented in this paper, kinetic fractionation during gas formation or inheritance from the kerogen cannot account for the observed variations. Hydrous pyrolysis experiments on two different shales have shown that ethane with a range of $\Delta^{13}C_2H_6$ can be created by the cracking processes. Although our dataset is limited, this indicates that ethane from different source rock types or maturation scenarios will have different $\Delta^{13}C_2H_6$.

The complete range of $\Delta^{13}C_2H_6$ in our suites cannot however be explained in that fashion. Fractionation occurring after cracking is necessary. Kinetic isotope effects associated with secondary cracking of ethane are a potential explanation. This is supported by a dry pyrolysis of ethane experiment. Using the experimental data, we have shown that up to 90% of the original ethane had been destroyed in the analysed samples. Ethane cracking was starting at low temperature (below 200°C), and before the co-existent oil was fully removed. The doubly-^{13}C-substituted ethane displays variations in natural materials that can constraint the evolution of natural gases due to kinetic processes after cracking.

Acknowledgements

This study was made possible through financial support of the NSF-EAR program, Petrobras and ExxonMobil. We are grateful to thank A. Sessions (Caltech) and Y. Tang (PEERI) for allowing us to make measurements in their laboratories.

Appendix

A. Limits to the determination of absolute clumping signatures

As said in the main text, we cannot create thermodynamically equilibrated ethane to anchor our measurements to an absolutely known isotopic composition. Another solution, as was done for the Pee Dee Belemnite, is to add known amounts of a labelled substance and to measure the isotopic compositions of the mixtures to extrapolate the exact amount of heavy isotope in the reference material. In our case, we will however show that this is not a workable solution.

An important source of error in the present case is the exact amount of labelled gas added to the reference gas. We should aim to add amounts of the labelled gas leading to increases in the measured $\Delta^{13}C_2H_6$ of 100‰ or less. The amount of $^{13}C_2H_6$ in the reference gas is about $10^{(-4)}$ compared to the amount of $^{12}C_2H_6$. Therefore to a mol of reference gas, we should add a few micromols of the reference gas to obtain the desired range in $\Delta^{13}C_2H_6$. Due to practical constrains (calibration of pressure gauges and significant digits displayed, calibration of the volumes in the vacuum line), this means that at best we know the relative amount of gas added to ±2%.

For a given amount of labelled gas added, we can calculate the $\Delta^{13}C_2H_6$ that would be measured on the mass spectrometer with the following equation:

$$\Delta^{13}C_2H_{6\,\mathrm{measured}} = 1000 \text{ x } (({}^{13}C_2H_{6\,\mathrm{ref}} + {}^{13}C_2H_{6\,\mathrm{added}}) \;/\; {}^{13}C_2H_{6\,\mathrm{ref}} - 1)$$

which can be reduced to

$$\Delta^{13}C_2H_{6\,\mathrm{measured}} = 1000 \text{ x } {}^{13}C_2H_{6\,\mathrm{added}} \;/\; {}^{13}C_2H_{6\,\mathrm{ref}}$$

A series of gas mixtures with different amounts of label added will form

a line in $\{\text{amount}_{\text{added}} - \Delta^{13}C_2H_6\}$ space, whose intercept is 0 and whose slope is proportional to the inverse of $^{13}C_2H_{6\,\text{ref}}$. To estimate the error on the determination of the amount of $^{13}C_2H_6$ in the reference gas, we ran a Monte-Carlo simulation of the calculation, with the following parameters:

- we assume for the sake of the calculation that we know the concentration of $^{13}C_2H_6$ exactly in the reference gas,
- 5 gas mixtures are created, with ideally $\Delta^{13}C_2H_6$ values of 10, 20, 30, 40 and 50‰, but a Gaussian error of ±2% on the amount of labelled gas really added,
- the $\Delta^{13}C_2H_6$ values of the mixtures are measured with a precision of ±0.1‰ (the limits of the methods presented in this paper)

With this scenario, the proportion of $^{13}C_2H_6$ in the reference gas would be known to ≈± 10‰, which is not a useful constrain given the precision of our methods.

Bibliography

Abelson, P. H., Hoering, T., 1961. Carbon isotope fractionation in formation of amino acids by photosynthetic organisms. Proceedings of the National Academy of Sciences of the United States of America 47 (5), 623.

Affek, H., Eiler, J., 2006. Abundance of mass 47 CO_2 in urban air, car exhaust, and human breath. Geochimica et Cosmochimica Acta 70 (1), 1–12.

826 Affek, H. P., Xu, X., Eiler, J. M., 2007. Seasonal and diurnal variations of
827 $^{13}C^{18}O^{16}O$ in air: Initial observations from Pasadena, CA. Geochimica et
828 Cosmochimica Acta 71 (21), 5033–5043.

829 Berndt, M., Seal, R., Shanks, W., Seyfried Jr., W., May 1996. Hydrogen
830 isotope systematics of phase separation in submarine hydrothermal sys-
831 tems: Experimental calibration and theoretical models. Geochimica et
832 Cosmochimica Acta 60 (9), 1595–1604.

833 Bigeleisen, J., Mayer, M. G., 1947. Calculation of equilibrium constants for
834 isotopic exchange reactions. The Journal of Chemical Physics 15 (5), 261–
835 267.

836 Burruss, R., Laughrey, C., 2010. Carbon and hydrogen isotopic reversals
837 in deep basin gas: Evidence for limits to the stability of hydrocarbons.
838 Organic Geochemistry 41 (12), 1285–1296.

839 Chung, H., Gormly, J., Squires, R., 1988. Origin of gaseous hydrocarbons
840 in subsurface environments: theoretical considerations of carbon isotope
841 distribution. Chemical Geology 71 (1), 97–104.

842 Clayton, C., 1991. Carbon isotope fractionation during natural gas generation
843 from kerogen. Marine and Petroleum Geology 8 (2), 232–240.

844 Dai, J., Xia, X., Li, Z., Coleman, D. D., Dias, R. F., Gao, L., Li, J., Deev,
845 A., Li, J., Dessort, D., et al., 2012. Inter-laboratory calibration of natural
846 gas round robins for δ^2H and $\delta^{13}C$ using off-line and on-line techniques.
847 Chemical Geology 310, 49–55.

de Matos, R. M. D., 1992. The northeast brazilian rift system. Tectonics 11 (4), 766–791.

DeNiro, M. J., Epstein, S., Jul. 1977. Mechanism of carbon isotope fractionation associated with lipid synthesis. Science 197 (4300), 261–263.

Dennis, K. J., Affek, H. P., Passey, B. H., Schrag, D. P., Eiler, J. M., 2011. Defining an absolute reference frame for 'clumped' isotope studies of CO_2. Geochimica et Cosmochimica Acta 75 (22), 7117–7131.

dos Santos Neto, E. V., Hayes, J. M., 1999. Use of hydrogen and carbon stable isotopes characterizing oils from the potiguar basin (onshore), northeastern brazil. AAPG bulletin 83 (3), 496–518.

Eiler, J. M., 2007. "Clumped-isotope" geochemistry—the study of naturally-occurring, multiply-substituted isotopologues. Earth and Planetary Science Letters 262 (3), 309–327.

Eiler, J. M., 2011. Paleoclimate reconstruction using carbonate clumped isotope thermometry. Quaternary Science Reviews 30 (25), 3575–3588.

Eiler, J. M., 2013. The isotopic anatomies of molecules and minerals. Annual Review of Earth and Planetary Sciences 41, 411–441.

Eiler, J. M., Clog, M., Magyar, P., Piasecki, A., Sessions, A., Stolper, D., Deerberg, M., Schlueter, H.-J., Schwieters, J., 2013. A high-resolution gas-source isotope ratio mass spectrometer. International Journal of Mass Spectrometry 335, 45–56.

869 Eiler, J. M., Schauble, E., 2004. $^{18}O^{13}C^{16}O$ in Earth's atmosphere. Geochim-
870 ica et Cosmochimica Acta 68, 4767–4777.

871 Fu, Q., Lollar, B. S., Horita, J., Lacrampe-Couloume, G., Seyfried, W. E.,
872 2007. Abiotic formation of hydrocarbons under hydrothermal conditions:
873 Constraints from chemical and isotope data. Geochimica et Cosmochimica
874 Acta 71 (8), 1982–1998.

875 Ghosh, P., Eiler, J., Campana, S. E., Feeney, R. F., Jun. 2007. Calibra-
876 tion of the carbonate "clumped isotope" paleothermometer for otoliths.
877 Geochimica et Cosmochimica Acta 71 (11), 2736–2744.

878 Gilbert, A., Robins, R. J., Remaud, G. S., Tcherkez, G. G., 2012. Intramolec-
879 ular 13c pattern in hexoses from autotrophic and heterotrophic c3 plant
880 tissues. Proceedings of the National Academy of Sciences 109 (44), 18204–
881 18209.

882 Hammes, U., Hamlin, H. S., Ewing, T. E., 2011. Geologic analysis of the
883 upper jurassic haynesville shale in east texas and west louisiana. AAPG
884 bulletin 95 (10), 1643–1666.

885 Kenney, J., Kutcherov, V. A., Bendeliani, N. A., Alekseev, V. A., 2002. The
886 evolution of multicomponent systems at high pressures: VI. the thermody-
887 namic stability of the hydrogen–carbon system: The genesis of hydrocar-
888 bons and the origin of petroleum. Proceedings of the National Academy of
889 Sciences 99 (17), 10976–10981.

890 Lash, G. G., Engelder, T., 2011. Thickness trends and sequence stratigraphy

of the middle devonian marcellus formation, appalachian basin: Implications for acadian foreland basin evolution. AAPG bulletin 95 (1), 61–103.

Lewan, M., Ruble, T., 2002. Comparison of petroleum generation kinetics by isothermal hydrous and nonisothermal open-system pyrolysis. Organic Geochemistry 33 (12), 1457–1475.

Mango, F. D., 1996. Transition metal catalysis in the generation of natural gas. Organic Geochemistry 24 (10), 977–984.

Martini, A., Walter, L., Budai, J., Ku, T., Kaiser, C., Schoell, M., 1998. Genetic and temporal relations between formation waters and biogenic methane: Upper Devonian Antrim Shale, Michigan Basin, USA. Geochimica et Cosmochimica Acta 62 (10), 1699–1720.

Mello, M., Telnaes, N., Gaglianone, P., Chicarelli, M., Brassell, S., Maxwell, J., 1988. Organic geochemical characterisation of depositional palaeoenvironments of source rocks and oils in brazilian marginal basins. Organic geochemistry 13 (1-3), 31–45.

Monson, K., Hayes, J., Feb. 1982. Carbon isotopic fractionation in the biosynthesis of bacterial fatty acids. ozonolysis of unsaturated fatty acids as a means of determining the intramolecular distribution of carbon isotopes. Geochimica et Cosmochimica Acta 46 (2), 139–149.

Piasecki, A., 2015. Site-specific isotopes in small organic molecules. Ph.D. thesis, California Institute of Technology.

Prinzhofer, A., Neto, E. V. D. S., Battani, A., 2010. Coupled use of carbon isotopes and noble gas isotopes in the potiguar basin (brazil): Fluids

migration and mantle influence. Marine and Petroleum Geology 27 (6), 1273–1284.

Prinzhofer, A., Pernaton, E., 1997. Isotopically light methane in natural gas: bacterial imprint or diffusive fractionation? Chemical Geology 142 (3), 193–200.

Prinzhofer, A. A., Huc, A. Y., 1995. Genetic and post-genetic molecular and isotopic fractionations in natural gases. Chemical Geology 126 (3), 281–290.

Robison, C. R., 1997. Hydrocarbon source rock variability within the austin chalk and eagle ford shale (upper cretaceous), east texas, usa. International Journal of Coal Geology 34 (3), 287–305.

Rudolph, J., 1995. The tropospheric distribution and budget of ethane. Journal of Geophysical Research: Atmospheres (1984–2012) 100 (D6), 11369–11381.

Schoell, M., 1983. Genetic characterization of natural gases. AAPG bulletin 67 (12), 2225–2238.

Slobod, R., 1951. Low temperature separation of ethane from methane and air. Analytical Chemistry 23 (2), 361–363.

Stolper, D., Lawson, M., Davis, C., Ferreira, A., Neto, E. S., Ellis, G., Lewan, M., Martini, A., Tang, Y., Schoell, M., et al., 2014b. Formation temperatures of thermogenic and biogenic methane. Science 344 (6191), 1500–1503.

Stolper, D., Martini, A., Clog, M., Douglas, P., Shusta, S., Valentine, D., Sessions, A., Eiler, J., 2015. Distinguishing and understanding thermogenic and biogenic sources of methane using multiply substituted isotopologues. Geochimica et Cosmochimica Acta 161, 219–247.

Stolper, D., Sessions, A., Ferreira, A., Neto, E. S., Schimmelmann, A., Shusta, S., Valentine, D., Eiler, J., 2014a. Combined ^{13}C–D and D–D clumping in methane: Methods and preliminary results. Geochimica et Cosmochimica Acta 126, 169–191.

Tang, Y., Huang, Y., Ellis, G. S., Wang, Y., Kralert, P. G., Gillaizeau, B., Ma, Q., Hwang, R., 2005. A kinetic model for thermally induced hydrogen and carbon isotope fractionation of individual n-alkanes in crude oil. Geochimica et Cosmochimica Acta 69 (18), 4505–4520.

Tang, Y., Perry, J., Jenden, P., Schoell, M., 2000. Mathematical modeling of stable carbon isotope ratios in natural gases. Geochimica et Cosmochimica Acta 64 (15), 2673–2687.

Urey, H. C., 1947. The thermodynamic properties of isotopic substances. J. chem. Soc., 562–581.

Vandenbroucke, M., Largeau, C., 2007. Kerogen origin, evolution and structure. Organic Geochemistry 38 (5), 719–833.

Wang, Z., Schauble, E. A., Eiler, J. M., 2004. Equilibrium thermodynamics of multiply substituted isotopologues of molecular gases. Geochimica et Cosmochimica Acta 68 (23), 4779–4797.

Whiticar, M., 1994. Correlation of natural gases with their sources. In: L.B. Magoon., W.G. Dow (Eds.), The Petroleum System—From Source to Trap, Memoir. Vol. 60. AAPG, Tulsa, pp. 261–283.

Yeung, L. Y., 2016. Combinatorial effects on clumped isotopes and their significance in biogeochemistry. Geochimica et Cosmochimica Acta 172, 22 – 38.

Yeung, L. Y., Young, E. D., Schauble, E. A., 2012. Measurements of $^{18}O^{18}O$ and $^{17}O^{18}O$ in the atmosphere and the role of isotope-exchange reactions. Journal of Geophysical Research: Atmospheres (1984–2012) 117 (D18).

Zumberge, J., Ferworn, K., Brown, S., 2012. Isotopic reversal ('rollover') in shale gases produced from the Mississippian Barnett and Fayetteville formations. Marine and Petroleum Geology 31 (1), 43–52.

7. Tables

1. *Table 1*

Isotopomers of ethane

Cardinal mass	Isotopomer	Proportion* (relative to C_2H_6)	Mass (a.m.u)
30	$^{12}CH_3$-$^{12}CH_3$	$9.77.10^{-1}$	30.047
31	$^{13}CH_3$-$^{12}CH_3$	$2.22.10^{-2}$	31.050
31	$^{12}CDH_2$-$^{12}CH_3$	$9.13.10^{-4}$	31.053
32	$^{13}C_2H_6$	$1.26.10^{-4}$	32.054
32	$^{13}CDH_2$-$^{12}CH_3$	$1.04.10^{-5}$	32.057
32	$^{13}CH_3$-$^{12}CDH_2$	$1.04.10^{-5}$	32.057
32	$^{12}CD_2H$-$^{12}CH_3$	$1.42.10^{-7}$	32.060
32	$^{12}CDH_2$-$^{12}CDH_2$	$2.13.10^{-7}$	32.060
33	$^{13}CDH_2$-$^{13}CH_3$	$1.18.10^{-7}$	33.060
33	$^{13}CD_2H$-$^{12}CH_3$	$1.62.10^{-9}$	33.063
33	$^{13}CDH_2$-$^{12}CDH_2$	$4.85.10^{-9}$	33.063
33	$^{13}CH_3$-$^{12}CD_2H$	$1.62.10^{-9}$	33.063
33	^{12}CD3-$^{12}CH_3$	$7.39.10^{-12}$	33.066
33	$^{12}CD_2H$-$^{12}CDH_2$	$6.65.10^{-11}$	33.066

2. *Table 2*

Comparison of values measured on a bottle of enriched gas used as an internal standard over 12 months. [a] : samples measured in a single analytical session.

$\delta^{13}C$	err	δD	err	$\Delta^{13}C_2H_6$	err
(‰)	(‰)	(‰)	(‰)	(‰)	(‰)
-10.95[a]	0.02	-115.63	0.52	-1.06	0.11
-10.97[a]	0.02	-114.35	0.80	-0.97	0.13
-10.98[a]	0.03	-114.70	0.72	-0.86	0.11
-10.95	0.02	-115.88	0.56	-0.94	0.13
-10.95	0.01	-116.32	0.38	-0.87	0.10
-10.9	0.03	-115.45	0.72	-0.96	0.12
-10.91	0.02	-116.13	0.56	-1.08	0.13
-10.9	0.05	-116.00	1.22	-1.07	0.14
-10.96	0.03	-115.39	0.70	-0.98	0.13

3. Table 3

Isotopic compositions measured for ethane samples of the 5 sample suites. The gas wetness is the molar ratio of gaseous alkanes heavier than methane to all gaseous alkanes. In locations, P refers to the Potiguar basin and SA to the Sergipe-Alagoas basin, H to Haynesville, M to Marcellus, EG to Eagle Ford. [a]: temperatures are from methane clumped isotopes in Stolper et al. (2014b). All the Sergipe-Alagoas samples were measured twice, in two different analytical sessions.

Sample	δD (‰)	error (‰)	δ^{13}C (‰)	error (‰)	$\Delta^{13}C_2H_6$ (‰)	error (‰)	Gas wetness	T[a] (°C)	error (°C)	Location
H1	-109.7	1.5	-19.3	0.07	-1.7	0.18	0.04	198	21	H
H2	-109.6	1.5	-20.8	0.07	-1.9	0.20	0.06			H
M1	-183.5	1.5	-40.3	0.06	-3.5	0.21	0.03			M
M2	-189.1	1.5	-42.3	0.08	-4.0	0.25	0.03	207	22	M
M3	-179.4	1.5	-38.2	0.06	-0.7	0.16	0.02	179	18	M
PT1	-110.3	1.5	-30.99	0.07	-2.4	0.25	0.15	221	24	P
PT2	-190.6	1.5	-39.81	0.07	0.37	0.19	0.41	167	18	P
PT3	-156.7	1.5	-34.99	0.06	0.60	0.25	0.27	182	18	P
PT4	-136.0	1.5	-30.64	0.13	-0.99	0.33	0.22	169	18	P
PT5	-209.1	1.5	-41.86	0.06	-2.72	0.30	0.14	157	15	P
PT7	-180.0	1.5	-35.08	0.13	-0.78	0.34	0.15	200	21	P
PT9	-133.8	1.5	-31.65	0.06	0.77	0.23	0.20	214	23	P
PT10	-124.9	0.8	-30.81	0.03	0.09	0.18	0.13			SA
PT11	-123.2	0.4	-32.16	0.02	0.17	0.08	0.16			SA
PT12	-129.3	0.9	-29.56	0.04	0.25	0.12	0.15			SA
PT13	-128.6	0.3	-32.20	0.01	-0.24	0.08	0.09			SA
PT14	-97.5	0.5	-27.49	0.01	-0.51	0.18	0.04			SA
EG1	-152.1	0.8	-32.75	0.33	0.83	0.19	0.30			EG
EG2	-159.0	0.5	-32.26	0.02	0.03	0.13	0.19			EG
EG3	-156.2	0.4	-32.66	0.01	-0.16	0.17	0.21			EG
EG4	-155.6	1.0	-32.57	0.04	-0.07	0.17	0.20			EG
EG5	-105.9	0.6	-24.80	0.02	-0.02	0.14	0.19			EG
EG6	-109.5	0.8	-24.32	0.02	-0.33	0.16	0.18			EG
EG7	-105.1	0.6	-18.71	0.02	-0.35	0.17	0.04			EG
EG8	-99.4	0.5	-23.10	0.02	0.25	0.12	0.14			EG

4. Table 4

Isotopic compositions of the ethane produced (for the hydropyrolysis experiments) or left (for the ethane pyrolysis experiment) as well as the percentage of ethane left for the pyrolysis experiments. The samples from the Woodford s

Sample	$\delta^{13}C$ (‰)	error (‰)	δD (‰)	error (‰)	$\Delta^{13}C_2H_6$ (‰)	error (‰)		
Woodford Shale								
330C	-273.6	0.9	-38.07	0.04	-1.22	0.13		
360C	-274.7	0.5	-34.28	0.02	-1.28	0.14		
390C	-249.5	0.6	-31.15	0.03	-0.78	0.12		
Araripe Shale								
320C	-257.7	0.5	-36.99	0.02	-1.16	0.15		
340C	-242.1	0.6	-35.56	0.02	-2.21	0.16		
360C	-236.1	0.6	-35.23	0.03	-2.09	0.13		
Ethane pyrolysis							Ethane yield	+/-
Start	-110.1	0.6	-24.39	0.03	0.19	0.11	100.00%	-
4h 600C	-23.8	0.7	-18.60	0.02	-0.27	0.13	70.00%	5.00%
8h 600C	4.6	1.6	-18.38	0.04	-1.5	0.4	35.00%	5.00%

8. Figure captions

1. Figure 1

Isotopic compositions of an internal standard measured over the course of 12 months. Solid lines are the average of all measurements, dashed lines the 1 standard deviation envelope around the average.

2. Figure 2

a) $\Delta^{13}C_2H_6$ versus $\delta^{13}C$ for the natural sample suites; b) $\Delta^{13}C_2H_6$ versus temperatures calculated from methane clumped isotopes. Open squares: Potiguar basin, full squares: Sergipe-Alagoas, open triangles: Eagle Ford, open square: Marcellus, full circles: Haynesville.

3. Figure 3

$\Delta^{13}C_2H_6$ of ethane gas produced by sequential hydrous pyrolysis of the Woodford Shale (open squares) and of the Arirape Shale (full squares) at each temperature.

4. Figure 4

Results from the ethane pyrolysis experiment at 600°C: $\Delta^{13}C_2H_6$ versus $\delta^{13}C$.

5. Figure 5

$\Delta^{13}C_2H_6$ versus gas wetness. There is a strong linear correlation observed for the Sergipe-Alagoas samples, whereas the data from the Potiguar basin form a triangular wedge pointing towards low wetness and low $\Delta^{13}C_2H_6$. Symbols as in Figure 2. The dotted line with an arrow shows the expected

path of ethane which is thermally cracked, using the results shown in Figure 4. See text for details.

9. Figures

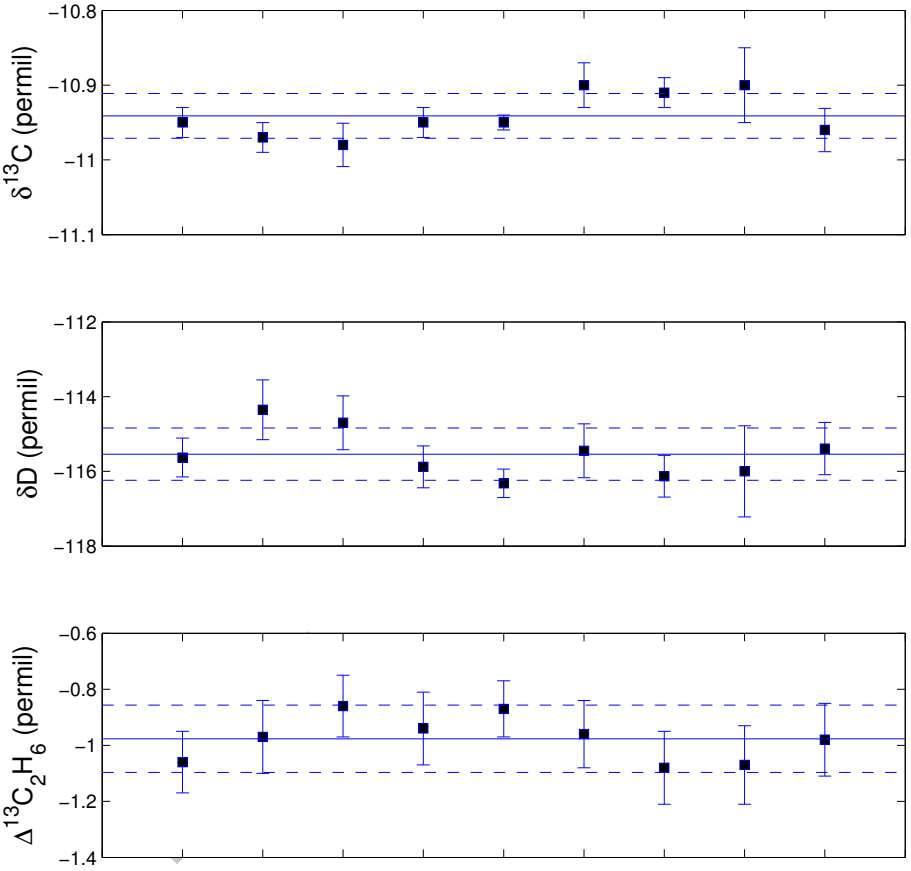

Figure 1: Figure 1.

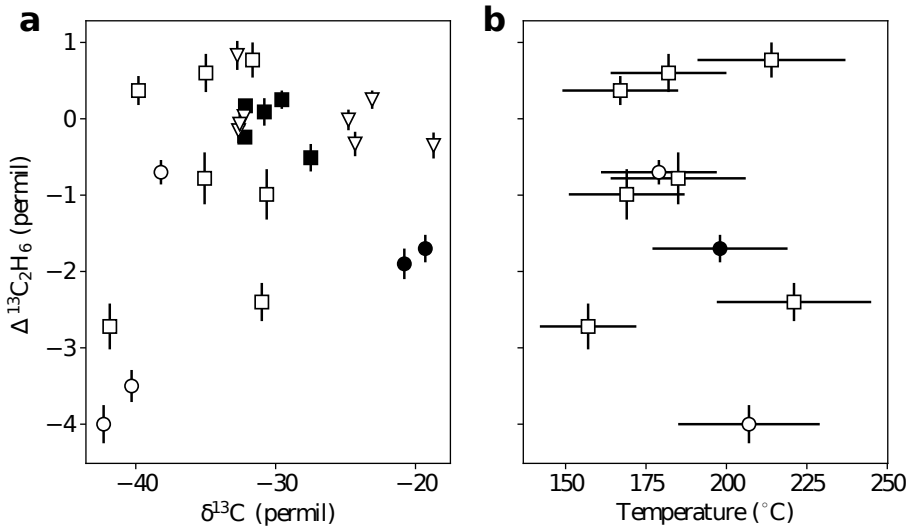

Figure 2: Figure 2.

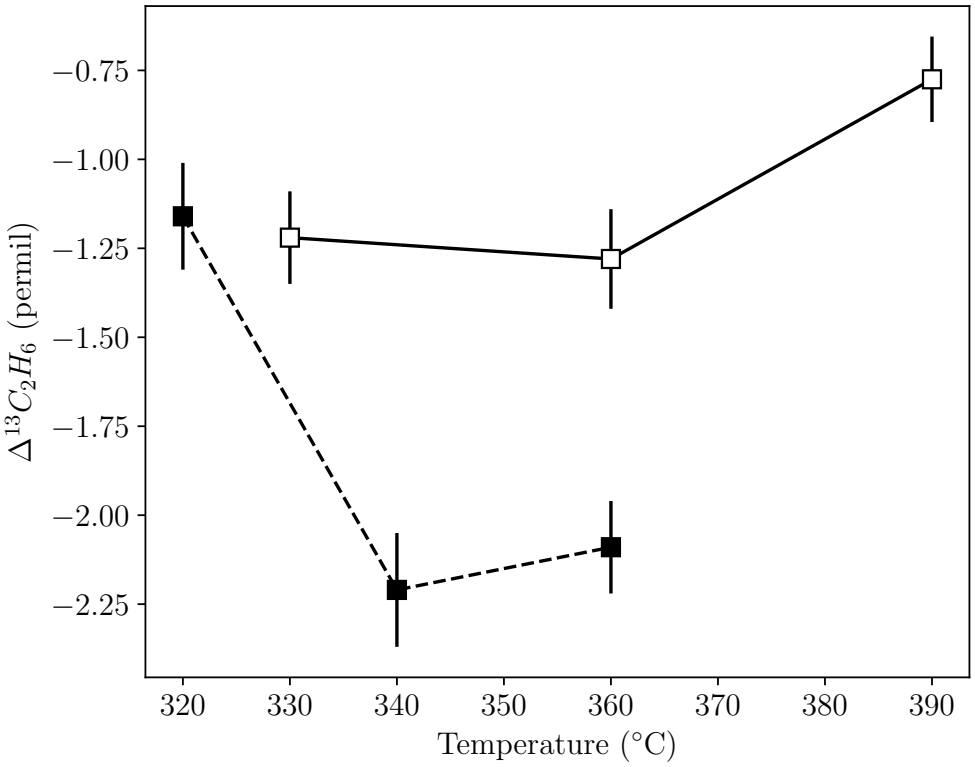

Figure 3: Figure 3.

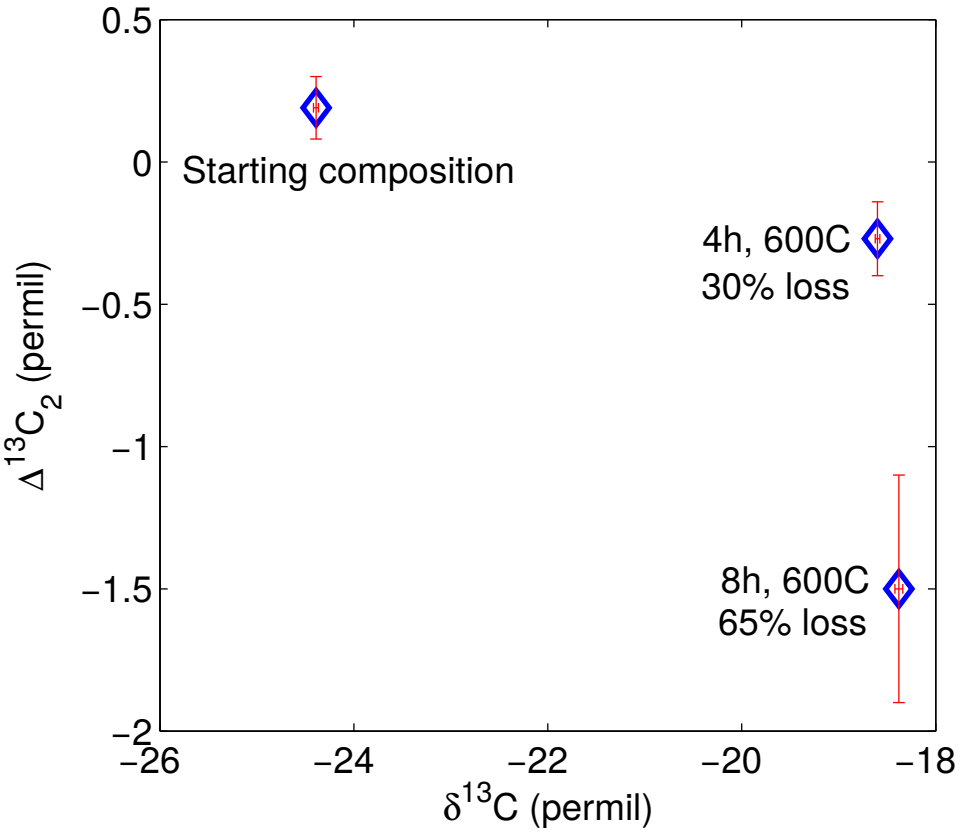

Figure 4: Figure 4.

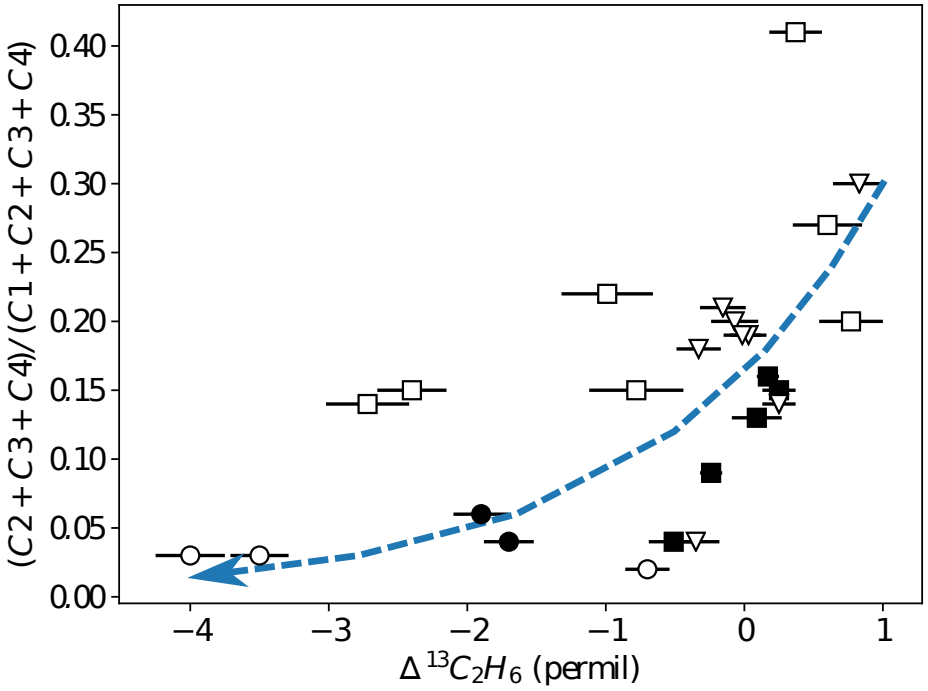

Figure 5: Figure 5.